Entry point into new trimeric and tetrameric imide-based macrocyclic esters derived from isophthaloyl dichloride and methyl 6-aminonicotinate

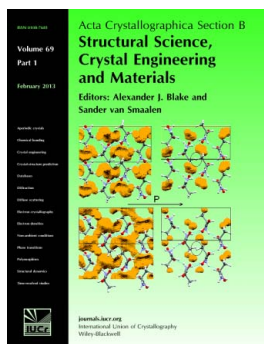Pavle Mocilac and John F. Gallagher

Acta Crystallographica Section B: Structural Science publishes papers in structural chemistry and solid-state physics in which structure is the primary focus of the work reported. The central themes are the acquisition of structural knowledge from novel experimental observations or from existing data, the correlation of structural knowledge with physico-chemical and other properties, and the application of this knowledge to solve problems in the structural domain. The journal covers metals and alloys, inorganics and minerals, metal-organics and purely organic compounds.

Crystallography Journals Online is available from journals.iucr.org

research papers

Entry point into new trimeric and tetrameric imide-based macrocyclic esters derived from isophthaloyl dichloride and methyl 6-aminonicotinate

Pavle Mocilac and John F. Gallagher*

School of Chemical Sciences, Dublin City University, Dublin 9, Ireland

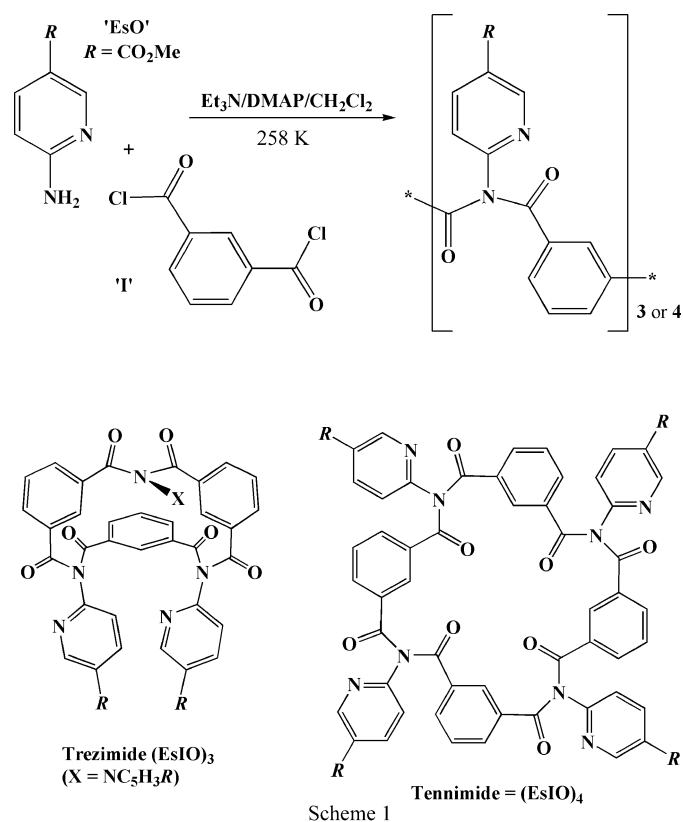Correspondence e-mail: john.gallagher@dcu.ie

The one-step reaction of isophthaloyl dichloride with the 2-aminopyridine derivative (methyl 6-aminonicotinate) yields (i) a trimer-based macrocycle $(EsIO)_3$ and (ii) a tetramer-based macrocycle $(EsIO)_4$ in modest isolated synthetic yields (total of 25%), together with (iii) longer open-chain oligomers. The macrocyclization relies on the semi-flexible imide *hinge* formed by reaction of the 2-amino(pyridine) functional group with two acyl chloride functional groups. The determining factors in macrocycle synthesis are: (*a*) imide formation using the heteroaromatic *ortho*-N functionality; (*b*) the inherent ability of the imide to twist by 85–115° from planarity (as measured by the CO$\cdots$CO imide torsion angles), thereby providing a *hinge* for macrocyclic ring closure or potentially (non)helical assembly in oligomer/polymer formation; (*c*) the conformational flexibility of the isophthaloyl group with *meta*-related carbonyl groups to twist and adopt either *syn* or *anti* conformations, although the *syn* conformation is observed structurally for all isophthaloyl groups in both $(EsIO)_3$ (trezimide) and $(EsIO)_4$ (tennimide) macrocycles.

1. Introduction

Natural and synthetic macrocycles continue to attract extensive scientific interest, with research developments proceeding in many directions including anion receptors, molecular recognition, drug discovery, therapeutics and nanoscience (Gloe, 2005; Vicens & Harrowfield, 2007; Driggers *et al.*, 2008; Steed & Atwood, 2009; Higson & Davis, 2011; Steed & Gale, 2012). Macrocyclic systems have evolved from the original crown ethers, spherands, cryptands and porphyrins, through calixarenes, resorcinarenes, rotaxanes, catenanes and beyond, as well as into interdisciplinary fields and biological applications (Evans & Gale, 2004; Driggers *et al.*, 2008; Steed & Gale, 2012). The quest to develop the *perfect* macrocyclic host template or platform with the ability to regulate specific physicochemical properties by simple functionalization remains the 'holy grail' of macrocyclic scientists. This on-going pursuit has yielded a diverse range of macrocyclic scaffolds over the past five decades, but has often been impeded by modest yields from multi-stage syntheses, using high-dilution techniques with complex separations and bearing necessary, but often redundant, backbone/side-chain groups (Steed & Gale, 2012).

Our research on the structural systematic studies of (1:1) benzamides shows that benzoyl-*N*-(2-pyridyl)benzamides are obtained as an additional (2:1) product when reacting benzoyl chlorides with 2-aminopyridines (O) (Gallagher *et al.*, 2009*a*,*b*; Mocilac *et al.*, 2010, 2012) where a second benzoyl chloride reacts with the amide (CONH) functionality yielding a (2:1) derivative (Lyon & Reese, 1974; Deady & Stillman, 1979;

Suzuki *et al.*, 1979). The (2:1) systems tend to adopt a distinct open and twisted geometry about the central imide '(O=C)$_2$NR' core as shown by their solid-state structures (R = 2-pyridyl; Gallagher *et al.*, 2009a,b; Mocilac *et al.*, 2010, 2012). Structural analysis demonstrates that these 2-(dibenzoylamino)pyridines constitute 3/8 of the '4 + 4' macrocyclic scaffold reported by Evans & Gale (2004), as derived from isophthaloyl dichloride (I) and either of the tetrafluoro F$_4$ and pentafluoroanilines F$_5$ (with a reasonable geometric fit of the non-H atoms). The sterically larger F$_4$ and F$_5$ while electronically favourable (for N—H deprotonation) may prevent trimer (trezimide) and limit tetramer (tennimide) formation due to the presence of the flanking *ortho*-F atoms. Synthetic strategies by us to synthesize the analogous 2-pyridyl-derived '4 + 4' macrocycles directly in one step using 2-aminopyridines (xO) and isophthaloyl dichloride (I) generates modest yields, though somewhat intractable product mixtures under a range of reaction conditions and reagents (Scheme 1), but from which both the previously unreported class of imide-based macrocyclic trimers (xIO)$_3$ and related tetramers (xIO)$_4$ (Figs. 1–3) can be isolated and characterized (xO = functionalized 2-aminopyridine, *e.g.* ester/acid/halide). Herein, when using methyl 6-aminonicotinate (as EsO), the cyclic triimide (EsIO)$_3$ (designated as a trezimide to distinguish it from known triimides; McMenimen & Hamilton, 2001; Gawroński *et al.*, 2002) and tetraimide (EsIO)$_4$ (designated as a tennimide from the tennis ball seam-line) have been isolated and characterized by spectroscopic techniques and single-crystal X-ray diffraction (Scheme 1, Figs. 2 and 3).

Scheme 1

Figure 1
Views of (*a*) the imide *hinge* CO···CO torsional twist angle; (*b*) the *syn-* and *anti-*conformations of the isophthaloyl groups; (*c*) the isophthaloyl OC···CO torsion angle and (*d*) the *cisoid* and *transoid* orientations of the *meta*-related isophthaloyl C=O groups.

2. Experimental

2.1. Materials and equipment

The vendors, analytical and spectroscopic equipment together with spectroscopic and computational methods used in this research are as reported previously (Gallagher *et al.*, 2010; Mocilac *et al.*, 2010, 2012; Mocilac, 2012).

2.2. Synthesis and characterization

The (EsIO)$_3$ and (EsIO)$_4$ macrocycles were synthesized from the (1:1) condensation of isophthaloyl dichloride (I) with methyl 6-aminonicotinate (EsO) in dry CH$_2$Cl$_2$ at 258 K using excess triethylamine (Et$_3$N) and a catalytic amount of dimethylaminopyridine (DMAP; Scheme 1; see supplementary material[1]). Both (EsIO)$_3$ and (EsIO)$_4$ were isolated in high purity from the reaction mixture using standard organic work-up (typically three washings of aqueous NH$_4$Cl solutions, pH $\simeq$ 5), dried over MgSO$_4$, filtered and dried to produce a yellow residue. The macrocycles were purified using standard column chromatography (silica gel, Davisil, 70 μm) and an eluant mixture of CHCl$_3$:EtOAc (1:1) to give the (EsIO)$_3$ (R_f = 0.60) and (EsIO)$_4$ (R_f = 0.33) as white solids in isolated yields of 16 and 9%, respectively.

(EsIO)$_3$ (m.p. 488–491 K): ^{1}H NMR, 600 MHz (CDCl$_3$, 294 K): δ 3.87 (3H, s, H27), 6.92 (1H, s, H26), 7.59 (1H, t, ^3J =

8 Hz, H15), 7.83 (1H, s, H12), 7.98 (2H, d, ^3J = 4 Hz, H14), 8.08 (1H, dd, ^3J = 4 Hz, ^4J = 2 Hz, H25), 8.53 (1H, s, H23). ^{13}C NMR: δ 52.63, 119.17, 123.91, 126.94, 130.74, 134.45, 134.60,

139.40, 150.30, 155.34, 164.58, 171.15. ATR-FTIR: 3079 (w), 2955 (w), 2848 (w), 1704 (s), 1593 (vs), 1476 (m), 1435 (m), 1380 (m), 1277 (s), 1247 (s), 1213 (s), 1194 (s), 1120 (s). ESI-MS (CH$_3$CN), M^+ = 846.75 g mol^{-1}. (EsIO)$_4$ (m.p. 474–478 K): ^{1}H NMR, 600 MHz (DMSO-d_6, 353 K): δ 3.91 (3H, H27), 7.17 (1H, H26), 7.77 (3H, H12, H15, H25), 7.99 (2H, H14), 8.11 (1H, H23). ^{13}C NMR (DMSO-d_6, 353 K): δ 52.55, 121.13, 124.16, 126.91, 130.81, 133.81, 134.02, 138.91, 149.41, 155.34, 163.85, 171.12. ATR-FTIR: 3091 (w), 3004 (w), 2956 (w), 2850 (w), 1715 (s), 1705 (s), 1694 (s), 1675 (s), 1591 (s), 1524 (w), 1476 (m), 1434 (m), 1383 (m), 1308 (sh), 1275 (s), 1215 (s), 1192 (m), 1167 (m), 1147 (m), 1119 (s). ESI-MS (CH$_3$CN), M^+ = 1129.0 g mol^{-1}.

2.3. Crystal structure determination, refinement and computing details

Crystals of (EsIO)$_3$ grow as very fragile, thin laths that diffract very weakly (Table 1). The first attempt (using Mo

(a)

(b)

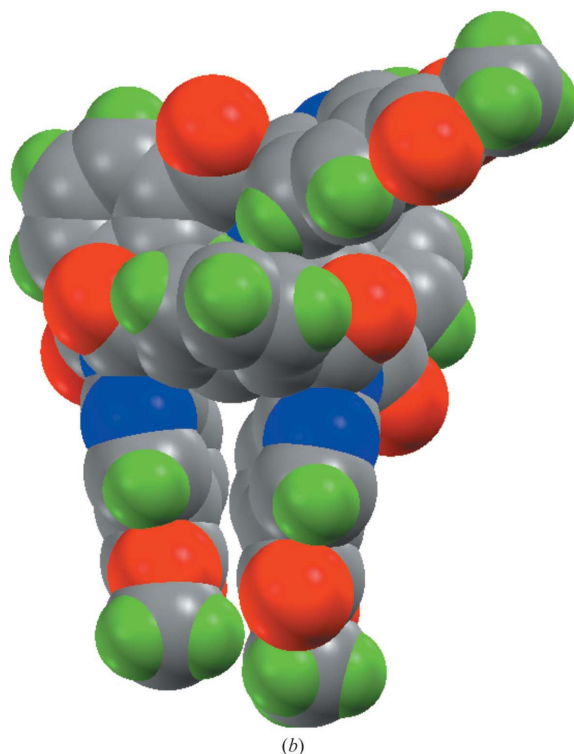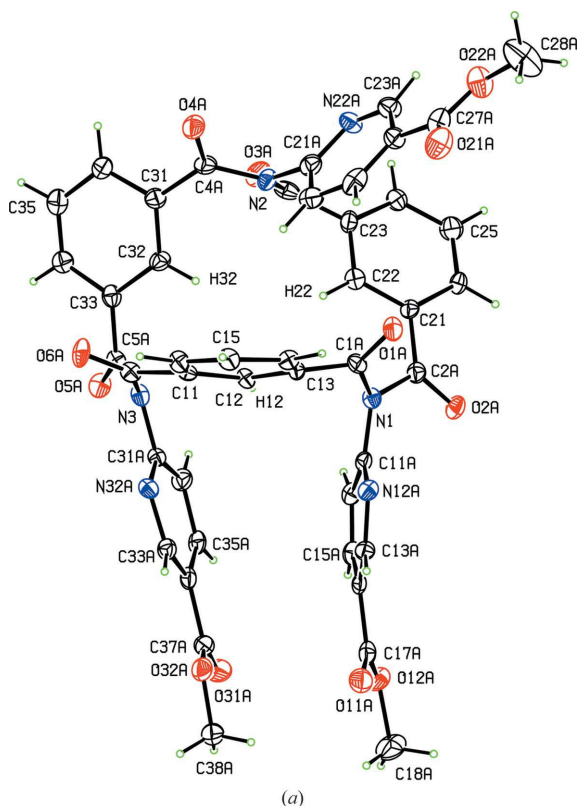**Figure 2**
View of (EsIO)$_3$ using (a) an ORTEP diagram of molecule A with non-H atoms depicted with 10% probability ellipsoids and (b) a similar view, with atoms as their van der Waal's spheres.

(a)

(b)

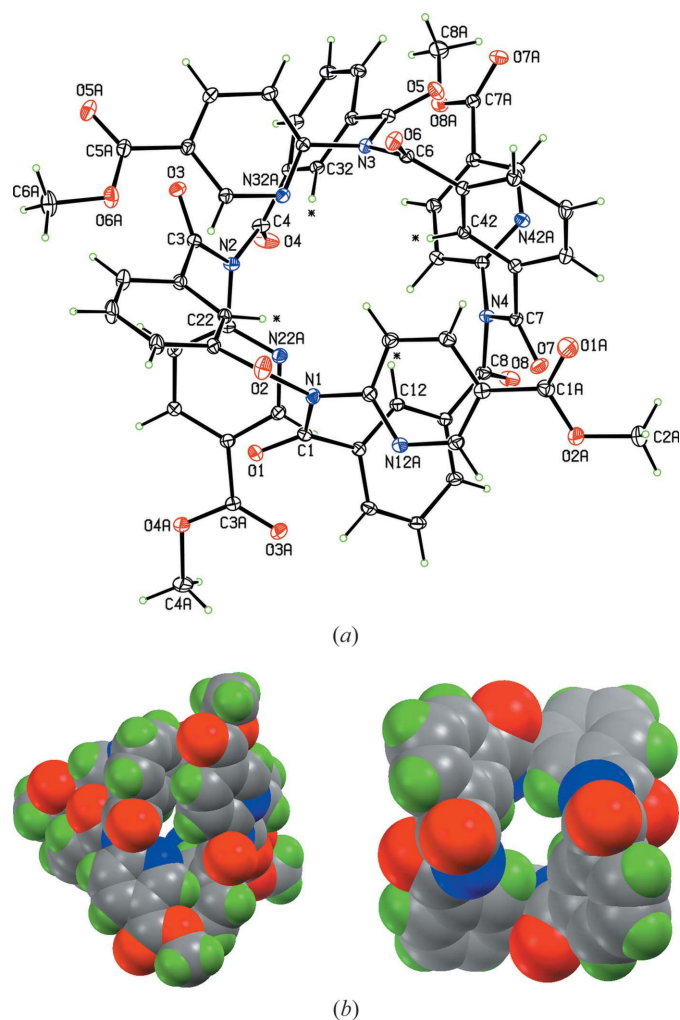**Figure 3**
Views of (EsIO)$_4$ using (a) an ORTEP diagram with non-H atoms depicted with 10% probability ellipsoids (the * highlighting the four isophthalic H atoms oriented towards the macrocyclic core) and (b) atoms as their van der Waal's spheres highlighting the molecular structure (left) and tennimide core (with the 2-pyridylcarboxylate moieties removed for visual effect).

Table 1
Experimental details.

For all structures: $Z = 4$. Experiments were carried out at 294 K with Cu $K\alpha$ radiation using a Xcalibur, Sapphire3, Gemini Ultra diffractometer. Analytical (ABSFAC; Clark & Reid, 1998). Refinement was with 0 restraints. H-atom parameters were constrained.

	(EsIO)$_3$†	(EsIO)$_4$
Crystal data		
Chemical formula	$C_{45}H_{30}N_6O_{12}$	$C_{60}H_{40}N_8O_{16}$
M_r	846.75	1129.00
Crystal system, space group	Triclinic, $P\bar{1}$ (No. 2)	Monoclinic, $P2_1/n$ (No. 14)
a, b, c (Å)	16.3411 (13), 16.5747 (4), 17.4806 (16)	10.6870 (1), 22.4852 (2), 22.6756 (2)
α, β, γ (°)	87.273 (5), 83.350 (7), 89.825 (4)	90, 101.721 (1), 90
V (Å^3)	4697.4 (6)	5335.31 (8)
μ (mm^{-1})	0.75	0.88
Crystal size (mm)	$0.60 \times 0.08 \times 0.015$	$0.58 \times 0.06 \times 0.05$
Data collection		
T_{min}, T_{max}	0.663, 0.989	0.631, 0.958
No. of measured, independent and observed [$I > 2\sigma(I)$] reflections	16 648, 10 048, 4137	31 765, 8619, 6947
R_{int}	0.083	0.034
θ_{max} (°)	51.4	63.3
$(\sin \theta/\lambda)_{max}$ (Å^{-1})	0.507	0.579
Refinement		
$R[F^2 > 2\sigma(F^2)]$, $wR(F^2)$, S	0.121, 0.352, 0.91	0.041, 0.120, 1.02
No. of reflections	10 048	8619
No. of parameters	1141	762
$\Delta\rho_{max}, \Delta\rho_{min}$ (e Å^{-3})	0.47, −0.35	0.27, −0.17

Computer programs: *CrysAlis PRO* (Agilent Technologies, Version 1.171.34.49, release 20-01-2011 CrysAlis171. NET, compiled Jan 20 2011, 15:58:25), *SHELXS*97, *SHELXL*97 (Sheldrick, 2008) and *PLATON* (Spek, 2009). † Crystals of (EsIO)$_3$ grow as thin laths from diethyl ether/*n*-hexane solutions. The crystals were very fragile and weakly diffracting. Data-collection strategies were devised to collect data to 1.0 Å resolution with a reflection cut-off point at 1.35 Å with $I > 3\sigma(I)$. The resulting data provided a solution using a moderate direct methods strategy. Attempts to obtain better quality crystals from a range of solvents were unsuccessful and crystals splintered easily on handling. The r.m.s. fit between molecules A and B is 0.60 Å in (EsIO)$_3$ as calculated from *PLATON* (Spek, 2009).

Table 2
Selected hydrogen bond and contact parameters (Å,°).

$D-H\cdots A$	$D-H$	$H\cdots A$	$D\cdots A$	$D-H\cdots A$
(EsIO)$_3$†				
$C28A-H28A\cdots O21A$	0.96	2.24	2.68 (2)	107
$C38A-H38A\cdots O31A$	0.96	2.19	2.630 (17)	107
$C35A-H35A\cdots O31A^{i}$	0.93	2.36	3.204 (13)	150
$C55A-H55\cdots O3A$	0.93	2.59	3.377 (14)	143
$C65A-H65A\cdots O61A^{ii}$	0.93	2.41	3.227 (14)	146
(EsIO)$_4$				
$C4A-H4A2\cdots O5^{iii}$	0.96	2.56	3.491 (4)	165
$C6A-H6A3\cdots O3^{iv}$	0.96	2.58	3.461 (4)	153
$C15A-H15A\cdots O4^{v}$	0.93	2.38	3.133 (3)	138
$C26A-H26A\cdots O5A^{iv}$	0.93	2.42	3.333 (3)	167
$C35A-H35A\cdots O7^{vi}$	0.93	2.57	3.107 (3)	117
$C36-H36\cdots O6^{vii}$	0.93	2.48	3.400 (2)	171

Symmetry codes: (i) $-x + 1, -y + 1, -z + 2$; (ii) $-x + 2, -y, -z$; (iii) $x - \frac{1}{2}, -y + \frac{1}{2}, z + \frac{1}{2}$; (iv) $-x, -y + 1, -z + 1$; (v) $x + 1, y, z$; (vi) $-x + \frac{1}{2}, y + \frac{1}{2}, -z + \frac{1}{2}$; (vii) $x - 1, y, z$. † The hydrogen-bond data (for both imide-based macrocycles) display a myriad of weaker C−H⋯O interactions with only the most important included in Table 2.

radiation) gave a unit cell and diffraction data to only 2.5 Å resolution, whereas a second data collection using Cu radiation gave observable reflection data to a 1.5 Å resolution limit

(although data were collected to 0.94 Å, using 1° ω scans, the detector positioned at 60 mm and with three shells collected for 16/48/48 s per frame). This dataset was not sufficient to produce a structural solution (data redundancy = 1.7, average F^2 = 2.1 and R_{int} = 0.16). Finally, on a third attempt, using Cu radiation at 40 kV, 40 mA over 72 h, observed reflection data were collected to a diffraction limit of 1.35 Å, frames to a 1.00 Å limit and with 0.5° scans per frame, shells collected for 24/48 s per frame and the detector at 60 mm (data redundancy = 1.8, average F^2 = 4.3 and R_{int} = 0.083). This dataset enabled a structural solution from a moderate direct methods attempt. It was obvious at an intermediate stage of the refinement that there were considerable voids in the lattice amounting to 21% of the unit cell containing solvent molecules of unknown composition and occupancy (from standard organic reaction work-up using several different solvents). The program *SQUEEZE* (Spek, 2009) was used (after several refinement attempts to determine the nature of the solvent type and site occupancy); the R factor dropped from 0.18 to 0.12 after using *SQUEEZE*. The subsequent full-matrix least-squares refinement proceeded without problems or the use of restraints on molecules A and B of (EsIO)$_3$ to give a satisfactory (EsIO)$_3$ crystal structure (with $Z' = 2$; Fig. 2). The high R factor (R = 0.12) is not uncommon in macrocycles with disorder and/or solvent molecules. The (EsIO)$_4$ macrocycle crystallized without solution or refinement problems, with no solvent or disorder in the crystal structure (Fig. 3).

All X-ray data were collected using Cu (or Mo initially) radiation on a Gemini S Ultra diffractometer at 294 K (Oxford Diffraction, 2011). Data reduction procedures and absorption corrections are standard and comprehensive details have been published elsewhere (Oxford Diffraction, 2011). All structures were solved using the *SHELXS*97 direct methods program (Sheldrick, 2008) and refined by full-matrix least-squares calculations on F^2 with all non-H atoms having anisotropic displacement parameters. H atoms were treated as riding atoms using the *SHELXL*97 defaults (Sheldrick, 2008, at 294 K). Selected crystallographic and structural information are provided in Tables 1–3 and supplementary material. Molecular diagrams (Figs. 2 and 3) were generated using *Mercury* (Macrae *et al.*, 2008) and crystal structure analysis using *PLATON* (Spek, 2009).

Table 3
Selected torsion angles in the imide *hinge* and isophthaloyl functional groups (°).

All torsion angle data were calculated using *PLATON* (Spek, 2009).

	CO$\cdots$CO twist	Isophthaloyl group		OC$\cdots$CO torsion
(EsIO)$_3$ imide *hinge*				
O1A=C1$A\cdots$C2A=O2A	95.5 (13)	O1A=C1$A\cdots$C6A=O6A		−17.8 (18)
O3A=C3$A\cdots$C4A=O4A	−111.3 (14)	O2A=C2$A\cdots$C3A=O3A		40.4 (17)
O5A=C5$A\cdots$C6A=O6A	−91.9 (15)	O4A=C4$A\cdots$C5A=O5A		128.7 (14)†
O1B=C1$B\cdots$C2B=O2B	91.6 (14)	O1A=C1$A\cdots$C6A=O6A		−18.7 (17)
O3B=C3$B\cdots$C4B=O4B	−108.8 (15)	O2A=C2$A\cdots$C3A=O3A		50.7 (16)
O5B=C5$B\cdots$C6B=O6B	−94.5 (14)	O4A=C4$A\cdots$C5A=O5A		121.9 (17)†
(EsIO)$_4$ imide *hinge*				
O1=C1$\cdots$C2=O2	113.0 (3)	O2=C2$\cdots$C3=O3		9.6 (3)
O3=C3$\cdots$C4=O4	−112.5 (3)	O4=C4$\cdots$C5=O5		2.5 (3)
O5=C5$\cdots$C5=O6	94.3 (3)	O6=C6$\cdots$C7=O7		6.2 (3)
O7=C7$\cdots$C8=O8	−88.9 (2)	O8=C8$\cdots$C1=O1		−25.4 (3)

† These OC$\cdots$CO angles are *transoid* compared with the other torsion angles (but are *syn*-related; Figs. 1*b*, *d*).

3. Results and discussion

3.1. Crystal and molecular structure of (EsIO)$_3$

Crystals of (EsIO)$_3$ were obtained as poor-quality laths from diethyl ether–*n*-hexane mixtures (though suitable for study by single-crystal X-ray diffraction to establish the molecular structure and geometry), whereas crystals of (EsIO)$_4$ grow as long needles from CHCl$_3$/MeOH solutions. The crystal structures of (EsIO)$_3$ and (EsIO)$_4$ are depicted in Figs. 2 and 3, respectively, and show several unique structural features. Imide formation presumably proceeds in a sequential fashion (in the absence of a template) by condensation of the substituted 2-aminopyridines with the aromatic dichloride and initially forming benzamides (Mocilac *et al.*, 2010, 2012) en route to imides (Lyon & Reese, 1974; Deady & Stillman, 1979; Suzuki *et al.*, 1979; Gallagher *et al.*, 2009*a,b*). On benzamide formation, the presence of the pyridyl *ortho*-N functionality assists in labilizing the amide N—H thus facilitating further condensation with a second isophthaloyl group and resulting in imide formation. In doing so, the tertiary imide N atom twists and rotates to accommodate both isophthaloyl groups such that the imide O=C$\cdots$C=O torsion angle twists away from planarity (Fig. 1*a*; denoted as the CO$\cdots$CO twist angle) in contrast to the relatively planar unsubstituted (OC)$_2$NH imide group. The labilizing effect of the *ortho*-N$_{pyridine}$ on the amide N—H in tandem with the less sterically hindered 2-aminopyridines (as compared with the tetra- and penta-fluoroanilines, F$_4$/F$_5$; Evans & Gale, 2004) drives the cyclization process in a sequential fashion using the imide group as a *hinge*. The (EsIO)$_3$ cyclization pathway utilizes the conformational semi-flexibility of the imide moiety, although the cyclization arises with some steric strain as shown by twisting of the scaffold C$_6$ rings and relative orientation of the isophthaloyl carbonyl groups; strain is relieved in producing the macrocyclic trimer. The formation of (EsIO)$_3$ can also be rationalized as the condensation of two [1 + 1] benzamide intermediates (each retaining reactive COCl and CONH groups); bridging using an isophthaloyl group forming two

imide linkages (*i.e.* at N1, N3) with macrocycle ring closure effected through the aminopyridine at N2 (Fig. 2*a*).

The (EsIO)$_3$ crystal structure ($Z' = 2$) crystallizes with small but significant differences between the two molecules (molecule *A*, Fig. 2). The (EsIO)$_3$ dataset facilitates analysis of the molecular geometry, however, some of the bond lengths are somewhat shorter than expected due to librational motion; the orientation of the 2-pyridinyl groups are for the most part unequivocal although there is an indication of disorder in one ring (at N5), but this was not treated due to the low data:parameter ratio and negligible effect on the structure. The (EsIO)$_3$ molecular conformation is unusual and represents the first *open-chain* macrocyclic imide trimer (trezimide) to be reported, although the structurally distinct rigid triimides are known (McMenimen & Hamilton, 2001; Gawroński *et al.*, 2002; Hanifi *et al.*, 2011). Molecules of (EsIO)$_3$ which are (syn)$_3$ with respect to their isophthaloyl groups (Fig. 1*b*) possess a macrocyclic *niche*. The three isophthalic H atoms H12, H22, H32 are oriented towards the macrocycle base with H$\cdots$H distances from 2.64 to 2.80 Å, whereas the carbonyl O atoms O2A, O3A and O5A (at the rim) are separated by distances of 5.76 to 7.92 Å (from molecule *A*, Fig. 2*a*). Two pyridine groups attached at N1 and N3 are oriented towards a parallel arrangement with their pyridyl *ortho*-N ring atoms N12A, N32A positioned *syn* (N12$A\cdots$N32A = 4.89 Å), and with their methyl carboxylates at contact distances (Fig. 2*b*). The pyridyl ring planes are oriented at angles of 30.2 (2) and 31.6 (2)° in molecules *A* and *B*, respectively, while their methyl carboxylates are approximately parallel at 1.75 (16) and 1.94 (14)°. The remaining pyridyl carboxylate at N2 is positioned on the opposite side of the molecular *niche*. A notable feature is that the imide O=C$\cdots$C=O torsion angles (as measured by the CO$\cdots$CO twist, Table 3; Fig. 1*a*) are in the range ±(90–110°) in (EsIO)$_3$ when compared with (EsIO)$_4$. The isophthaloyl OC$\cdots$CO torsion angles (Fig. 1*c*), however, adopt a wider range of values, thus highlighting the isophthaloyl group twisting and distortion that arises on cyclization (Table 3, Fig. 1*d*). The isophthaloyl carbonyl groups can adopt *syn/anti*-conformations and can also adopt *cisoid/transoid* arrangements (Figs. 1*b* and *d*). Differences reflect additional molecular strain in the trezimide (EsIO)$_3$ compared with the tennimide (EsIO)$_4$ as well as crystal-packing requirements. The ease with which the isophthaloyl groups can twist/distort in comparison with the imide *hinge* has been rationalized in terms of energy barriers which are considerably lower for the isophthaloyl groups (Mocilac, 2012). Hence, molecular strain is relieved with conformational change arising mainly in the isophthaloyl groups.

The (EsIO)$_3$ macrocycle comprises nine C=O, three pyridine N and three ester acceptor groups (neglecting the tertiary imide N1, N2 and N3 atoms oriented towards the macrocycle

niche) and is an acceptor-rich system in the absence of strong donor groups. Therefore, molecular aggregation in the crystal structure is dominated by the cumulative effect of several though relatively weak C—H⋯O=C interactions and contacts per macrocycle (Table 2) although some are not apparent due to the treatment of the lattice voids in refinement using *SQUEEZE* (Spek, 2009).

Analysis of (EsIO)$_3$ as the combination of basic 'benzamide' units demonstrates that it is a combination of units that resemble both regular benzamides (Kavallieratos *et al.*, 1997; Qin *et al.*, 2006; Mocilac *et al.*, 2010, 2012) and *N*-methylated amides used as molecular splints both in acycles and macrocycles (Yamaguchi *et al.*, 1991; Azumaya *et al.*, 2003). Macrocycles that are trimeric in nature for the most part tend to be symmetrical unless there is a particular geometrical feature that distorts or buckles the macrocycle towards asymmetry (Steed & Gale, 2012). (EsIO)$_3$ is inherently asymmetrical and especially with respect to the orientation of the pendant pyridyl side chains. As (EsIO)$_3$ represents the first trimeric macrocycle of its type, the development of its molecular scaffold (where the inherent asymmetry can be utilized for a particular application) is a key priority.

3.2. (EsIO)$_4$ crystal and molecular structure

The formation of (EsIO)$_4$ can be rationalized as condensation of two [1 + (1 + 2)] intermediates *via* the analogous (1:2) systems reported by Crabtree and co-workers in 1997 (*e.g.* RINGOK; Kavallieratos *et al.*, 1997; Allen & Motherwell, 2002) as distinct from the sequential addition of alternating I and EsO groups in a cyclic fashion (although not statistically favoured). A key feature to note in (EsIO)$_4$ is that the imide O=C⋯C=O torsion angles (as measured by the CO⋯CO twist) are in a relatively narrow range (85–115°) and specifically +113.0 (3), −112.5 (3), +94.3 (3) and −88.9 (2)° with differences reflecting molecular relaxation and crystal packing requirements. The isophthaloyl OC⋯CO torsion angles are 9.6 (3), 2.5 (3), 6.2 (3) and −25.4 (3)° and mostly orient in the same direction adopting a rather narrow range as compared with (EsIO)$_3$. The (EsIO)$_4$ molecular structure adopts a tetrahedral-like framework (Fig. 3) with the macrocyclic scaffold having a twisted saddle-like appearance and broadly similar to the IYUQUO/IYURAV, (IF$_5$)$_4$/(IF$_4$)$_4$ scaffolds (Evans & Gale, 2004; Allen & Motherwell, 2002). The (EsIO)$_4$ macrocyclic cavity is rather compact with H⋯H (* in Fig. 3*a*) intra-annular cross-cavity distances of 4.13 and 4.18 Å. The four tertiary imide N1/N2/N3/N4 atoms distort from planarity from the 3C atom plane (to which these N atoms are bonded, Fig. 1*a*) and by 0.113 (2) to 0.185 (2) Å (N⋯C$_3$) towards the macrocyclic cavity core; the tetrahedral-like cavity shape is demonstrated by the six tertiary imide N⋯N distances ranging from 5.27 to 5.34 Å (for four sides) and two longer separations at 5.72 and 5.89 Å. The molecular cavity is almost certainly too small to accommodate a small molecule, but under suitable conditions and with macrocyclic flexibility may be able to accommodate a cation, *e.g.* Li$^+$, Na$^+$ although this would need to arise at the cyclization stages. There are several

C—H⋯O=C intermolecular interactions of note which assist in aggregation and crystal structure formation and the most important of these involve the C15*A*, C26*A* and C36 atoms as donors (Table 2). There are several differences between the fluorinated tennimides (Evans & Gale, 2004) and (EsIO)$_4$ stemming principally from the effect of the less bulky pyridyl side chains (EsO) that presumably facilitates both relative ease of synthesis, cyclization, separation and isolated yields. In IYUQUO/IYURAV (Evans & Gale, 2004) the effect of the phenyl ring fluoro substituents can be discerned by the slightly larger N⋯C3 plane separations from 0.13 to 0.19 Å, larger CO⋯CO twists (ranging from −101.5 to 120.5°) and isophthaloyl OC⋯CO torsion angles (ranging from −34.9 to 20.5°) in both macrocycles.

3.3. Solution NMR and spectroscopic studies of (EsIO)$_3$ and (EsIO)$_4$

Solution NMR studies of (EsIO)$_3$ and (EsIO)$_4$ can readily distinguish both macrocycles and reveal the symmetrical nature of the latter (tennimide) in comparison to the former (trezimide). (EsIO)$_3$ (in CDCl$_3$) shows greater conformational flexibility at 294 K compared with (EsIO)$_4$, however, the tennimide is relatively robust in solution at elevated temperatures during variable-temperature (VT) NMR studies, whereas the trezimide decomposes slowly in dimethylsulfoxide (DMSO). Analysis of (EsIO)$_4$ in DMSO-d_6 using variable-temperature NMR studies demonstrates that the macrocycle is relatively rigid and does not readily interconvert between a range of conformers at room temperature, but only at higher temperatures (peak resolution improves with increasing temperature during the VT run). The corresponding CDCl$_3$ data (294 K) highlights the relative inflexibility and 'locked' conformation of (EsIO)$_4$. IR (ATR) spectra shows the C=O peaks due to both imide and carboxylate moieties and are broadly similar for both macrocycles, whereas ESI-MS data indicates the molecular ions for both (EsIO)$_3$ and (EsIO)$_4$ with fragmentation due to CO$_2$Me (59) and major fragments including the C$_6$ and C$_5$N ring moieties.

3.4. Synthetic approach and future development

The one-step synthetic approach reported by Evans & Gale (2004) to produce both IYUQUO/IYURAV imide-based tetramers using fluorinated anilines is both an elegant example of self-templation in macrocyclic chemistry as well as providing a unique tetrameric scaffold unseen previously or since (Steed & Gale, 2012). It is, however, a modest-yielding synthetic route (∼10%). Statistical factors in combination with moisture-sensitive components and the relatively sterically hindered fluorinated phenyl rings (although electronically suitable for *N*-activation) combine to only produce the (IF$_{4/5}$)$_4$ prototype imide tetramers. The electron-withdrawing fluorinated aniline ring drives the deprotonation reaction but may also hinder trimer formation somewhat due to the bulkier, flanking 2,6-*ortho*-F atoms. Utilization of 2-aminopyridine derivatives (xO) (*e.g.* methyl 6-aminonicotinate) is

favoured both on steric (ability to rotate/twist/distort) and electronic grounds (*ortho*-N$_{pyridine}$) to produce new series of imide-based trezimides (xIO)$_3$ and tennimides (xIO)$_4$ (x = ester/acid/halide *etc.*). Additionally, tennimides can be synthesized exclusively *via* the 1:2 precursor (an analogue of YERZOL; Qin *et al.*, 2006) through condensation with isophthaloyl dichloride in a $2 \times [1 + (1 + 2)]$ synthesis. The advantages in using a one-step synthetic reaction instead of a multi-step approach are many fold (*i.e.* cost, time, green methodology) and this theme has been discussed recently in amide-linked pentamers (Ren *et al.*, 2011; Du *et al.*, 2011).

The (EsIO)$_3$ and (EsIO)$_4$ macrocycles have been synthesized in one step in modest yields (totalling 25%) in the absence of a template (Mocilac, 2012). Crystal structure analysis shows that the trezimide (EsIO)$_3$ adopts an open but highly asymmetric conformation with a small molecular *niche*, whereas the tennimide (EsIO)$_4$ adopts a twisted clasp-like conformation with a small macrocyclic core generated by macrocycle folding. For both (EsIO)$_3$ and (EsIO)$_4$, the semi-flexible (on steric grounds) imide linkage only adopts a relatively narrow range of torsion angles as measured by the imide CO$\cdots$CO angles of $\pm(85-115°)$. The isophthaloyl moiety, analysed by the OC$\cdots$CO angles, shows that all four pairs of O atoms are *cisoid* in (EsIO)$_4$, but two are *cisoid* and one is *transoid* in (EsIO)$_3$ reflecting the distinct isophthaloyl group twisting that is necessary to accommodate (EsIO)$_3$ formation (Table 3). The distinct molecular conformations suggest quite different potential applications for these macrocycles and related acycles/foldamers (Steed & Gale, 2012; Berl *et al.*, 2001*a,b*). The (EsIO)$_3$ trezimide with a molecular *niche* and two pyridine rings separated at contact distances may have potential in coordination chemistry. The use of pyridine and related heteroaromatic rings in macrocyclic chemistry has been extensive over the past few decades (Pappalardo *et al.*, 1992; Ferguson *et al.*, 1994; Steed & Gale, 2012). The flattened tetrahedral conformation of (EsIO)$_4$ with both an internal cavity (that can be potentially expanded) as well as external functional groups (pyridines, esters) suggests a rich future potential in both supramolecular and medicinal chemistry (Isidro-Llobet *et al.*, 2011).

4. Conclusion

The reaction of isophthaloyl dichloride (I) with functionalized 2-aminopyridines (xO) is quite general in applicability with a diverse range of macrocyclic derivatives that can be potentially synthesized and characterized from commercially available 2-aminopyridines, with pyrimidines currently being explored (Mocilac, 2012). The diverse range of carboxamide linkages that can be converted into an imide linkage *via* the *ortho*-pyridine group suggests a rich vein of chemistry lies ahead (Berl *et al.*, 2001*a,b*; Steed & Gale, 2012; Zhang *et al.*, 2012). We are presently exploring several facets of both types of trezimide and tennimide with a special interest in (i) varying the functionality of the heteroaromatic ring and (ii) understanding the nature of the imide 'CO$\cdots$CO' twist (imide

hinge): the results of these studies will be communicated shortly.

References

Allen, F. H. & Motherwell, W. D. S. (2002). *Acta Cryst.* B**58**, 407–422.

Azumaya, I., Okamoto, T., Imabeppu, F. & Takayanagi, H. (2003). *Tetrahedron*, **59**, 2325–2331.

Berl, V., Huc, I., Khoury, R. G. & Lehn, J. M. (2001*a*). *Chem. Eur. J.* **7**, 2798–2809.

Berl, V., Huc, I., Khoury, R. G. & Lehn, J. M. (2001*b*). *Chem. Eur. J.* **7**, 2810–2820.

Clark, R. C. & Reid, J. S. (1998). *Comput. Phys. Commun.* **111**, 243–257.

Deady, L. W. & Stillman, D. C. (1979). *Aust. J. Chem.* **32**, 381–386.

Driggers, E. M., Hale, S. P., Lee, J. & Terrett, N. K. (2008). *Nat. Rev. Drug Discov.* **7**, 608–624.

Du, Z. Y., Ren, C. L., Ye, R. J., Shen, J., Maurizot, V., Lu, Y. J., Wang, J. & Zeng, H. Q. (2011). *Chem. Commun.* **47**, 12488–12490.

Evans, L. S. & Gale, P. A. (2004). *Chem. Commun.* pp. 1286–1287.

Ferguson, G., Gallagher, J. F., Giunta, L., Neri, P., Pappalardo, S. & Parisi, M. (1994). *J. Org. Chem.* **59**, 42–53.

Gallagher, J. F., Alley, S., Brosnan, M. & Lough, A. J. (2010). *Acta Cryst.* B**66**, 196–205.

Gallagher, J. F., Donnelly, K. & Lough, A. J. (2009*a*). *Acta Cryst.* E**65**, o102–o103.

Gallagher, J. F., Donnelly, K. & Lough, A. J. (2009*b*). *Acta Cryst.* E**65**, o486–o487.

Gawroński, J., Brzostowska, M., Gawrońska, K., Koput, J., Rychlewska, U., Skowronek, P. & Nordén, B. (2002). *Chem. Eur. J.* **8**, 2484–2494.

Gloe, K. (2005). *Macrocyclic Chemistry, Current Trends and Future Perspectives.* Dordrecht, The Netherlands: Springer.

Hanifi, D., Cao, D., Klivansky, K. L. & Liu, Y. (2011). *Chem. Commun.* **47**, 3454–3456.

Higson, S. & Davis, F. (2011). *Macrocycles: Construction, Chemistry and Nanotechnology Applications.* New York: John Wiley and Sons Ltd.

Isidro-Llobet, A., Murillo, T., Bello, P., Cilibrizzi, A., Hodgkinson, J. T., Galloway, W. R., Bender, A., Welch, M. & Spring, D. R. (2011). *Proc. Natl Acad Sci. USA*, **108**, 6793–6798.

Kavallieratos, K., de Gala, S. R., Austin, D. J. & Crabtree, R. H. (1997). *J. Am. Chem. Soc.* **119**, 2325–2326.

Lyon, P. A. & Reese, C. B. (1974). *J. Chem. Soc. Perkin Trans. 1*, pp. 2645–2649.

Macrae, C. F., Bruno, I. J., Chisholm, J. A., Edgington, P. R., McCabe, P., Pidcock, E., Rodriguez-Monge, L., Taylor, R., van de Streek, J. & Wood, P. A. (2008). *J. Appl. Cryst.* **41**, 466–470.

McMenimen, K. A. & Hamilton, D. G. (2001). *J. Am. Chem. Soc.* **123**, 6453–6454.

Mocilac, P. (2012). PhD thesis. Dublin City University, Ireland.

Mocilac, P., Donnelly, K. & Gallagher, J. F. (2012). *Acta Cryst.* B**68**, 189–203.

Mocilac, P., Tallon, M., Lough, A. J. & Gallagher, J. F. (2010). *CrystEngComm*, **12**, 3080–3090.

Oxford Diffraction (2011). *ABSFAC* and *CrysAlisPro CCD/RED*, Version 1 171.34.49. Oxford Diffraction Ltd, Abingdon, Oxfordshire, UK.

Pappalardo, S., Giunta, L., Foti, M., Ferguson, G., Gallagher, J. F. & Kaitner, B. (1992). *J. Org. Chem.* **57**, 2611–2624.

Qin, D.-B., Jin, L.-H., Zhang, H.-X. & Gu, S-J. (2006). *Acta Cryst.* E**62**, o4519–o4520.

Ren, C., Maurizot, V., Zhao, H., Shen, J., Zhou, F., Ong, W. Q., Du, Z., Zhang, K., Su, H. & Zeng, H. (2011). *J. Am. Chem. Soc.* **133**, 13930–13933.

Sheldrick, G. M. (2008). *Acta Cryst.* A**64**, 112–122.

Spek, A. L. (2009). *Acta Cryst.* D**65**, 148–155.

Steed, J. W. & Atwood, J. L. (2009). *Supramolecular Chemistry*, 2nd ed. New York: John Wiley and Sons.

Steed, J. W. & Gale, P. A. (2012). *Supramolecular Chemistry: from Molecules to Nanomaterials*, Vols. 1–8, pp. 1–4014. New York: John Wiley and Sons.

Suzuki, T., Kenbou, N. & Mitsuhashi, K. (1979). *J. Heterocycl. Chem.* **16**, 645–648.

Vicens, J. & Harrowfield, J. (2007). *Calixarenes in the Nanoworld.* Dordrecht, The Netherlands: Springer.

Yamaguchi, K., Matsumura, G., Kagechika, H., Azumaya, I., Ito, Y., Itai, A. & Shudo, K. (1991). *J. Am. Chem. Soc.* **113**, 5474–5475.

Zhang, D.-W., Zhao, X., Hou, J.-L. & Li, Z.-T. (2012). *Chem. Rev.* **112**, 5271–5316.